IOPscience iopscience.iop.org

Home Search Collections Journals About Contact us My IOPscience

Polarization and self-polarization in thin $PbZr_{1-x}Ti_xO_3$ (PZT) films

This article has been downloaded from IOPscience. Please scroll down to see the full text article.

2001 J. Phys.: Condens. Matter 13 8755

(http://iopscience.iop.org/0953-8984/13/39/304)

View the table of contents for this issue, or go to the journal homepage for more

Download details:
IP Address: 171.66.16.226
The article was downloaded on 16/05/2010 at 14:54

Please note that terms and conditions apply.

INSTITUTE OF PHYSICS PUBLISHING JOURNAL OF PHYSICS: CONDENSED MATTER

J. Phys.: Condens. Matter **13** (2001) 8755–8763 PII: S0953-8984(01)18242-1

Polarization and self-polarization in thin $PbZr_{1-x}Ti_xO_3$ (PZT) films

V P Afanasjev[1], A A Petrov[1], I P Pronin[2], E A Tarakanov[2], E Ju Kaptelov[2] and J Graul[3]

[1] Electrotechnical University, Department of Microelectronics, Professor Popova Street, 5, 197376 St Petersburg, Russia
[2] Ioffe Physico-Technical Institute, Russian Academy of Sciences, Polytechnicheskaya, 26, 194021 St Petersburg, Russia
[3] University of Hannover, Laboratory for Information Technology, Schneiderberg 32, D-30167 Hannover, Germany

Received 23 October 2000, in final form 25 July 2001
Published 13 September 2001
Online at stacks.iop.org/JPhysCM/13/8755

Abstract

The self-polarization effect in ferroelectric thin films has been studied for PZT films 0.5–1 μm thick deposited by radio-frequency magnetron sputtering of various ferroelectric ceramic targets (Zr/Ti = 54/46, Zr/Ti = 54/46 + 10% PbO and Zr/Ti = 40/60 + 10% PbO). The laser intensity modulation method has been applied, together with the methods of C–V characteristics and dielectric hysteresis loops, to determine the polarization distribution and evaluate the built-in electric fields in the films. It is shown that the bottom interface of the thin-film Pt–PZT–Pt capacitor structure is the source of self-polarization for a certain technological sequence of structure formation. The self-polarization effect is caused by two factors: (i) n- or p-type conductivity due to oxygen or lead vacancies or other impurities in the films and (ii) high trap density at the bottom interface of the structure.

1. Introduction

Thin $PbZr_{1-x}Ti_xO_3$ (PZT) ferroelectric films are very promising for integrated pyroelectric IR sensor and MEMS applications. In particular, thin PZT films prepared by RF magnetron sputtering of ceramic targets and exhibiting self-polarization have attracted considerable interest with regard to fabrication of pyroelectric infrared sensor arrays. Self-polarized PZT films show high pyroelectric coefficients, in some cases comparable with those of films subjected to subsequent poling [1–3].

Self-polarization seems to be manifested in *in situ* grown thin films [1–6]. The data reported in [2–4] for such films reflect the existence of a strong internal bias field of 70 kV cm^{-1} and more. It has been suggested that the stronger the built-in field, the greater the self-polarization effect [5]. A strong self-polarization effect has been observed in tetragonal PZT

 © 2001 IOP Publishing Ltd Printed in the UK

films [2, 3]. By contrast, the effect vanishes in rhombohedral PZT films [3]. According to [6], the direction of self-polarization depends on the excess of lead oxide (PbO) in the ceramic target and changes to the opposite with increasing PbO content.

Different mechanisms giving rise to self-polarization are currently being discussed. One of these is associated with a Schottky barrier acting as a built-in field poling the interfacial region of a ferroelectric film [7–9]. It has been suggested that the interface gets charged owing to a high concentration of donor or acceptor traps [9–11]. In [11, 12], a significant effect of excess PbO on the density of interfacial charges was demonstrated. Nevertheless, the self-polarization mechanism has not been elucidated yet.

In this work, the self-polarization phenomenon in thin PZT films was studied using the laser intensity modulation method (LIMM), microstructural and compositional analyses (XRD and AES, respectively) and dielectric and pyroelectric techniques.

2. Experimental procedure

Experimental details of PZT film deposition have been reported previously [13, 14]. Thin PZT films were fabricated by RF magnetron sputtering of several ferroelectric ceramic targets of Zr/Ti = 54/46, Zr/Ti = 54/46 + 10% PbO and Zr/Ti = 40/60 + 10% PbO compositions. Amorphous films 0.5–1 μm thick were deposited at relatively low temperatures onto glass-ceramic, silicon and fused silica substrates with platinum as the bottom electrode. Platinum was also used as the top electrode. A perovskite structure was formed upon subsequent annealing at temperatures of 520–600 °C by an *ex situ* procedure. XRD and AES were applied to study the microstructure and composition of PZT films. LIMM measurements were used to examine the polarization distribution in relation to film thickness [15–18], together with investigations of P–E and C–V characteristics.

3. Results

Thin *ex situ* grown PZT films have polycrystalline perovskite structure [14]. Optical inspection of the phase homogeneity and XRD analysis [19] revealed no inclusions of non-perovskite phases exceeding their detection limits.

Figure 1 demonstrates AES profiles for PZT films. It is clearly seen that the distribution of elements across the film is homogeneous, which is characteristic of all the films under investigation. For PZT films grown by sputtering a target with excess of PbO and thermally

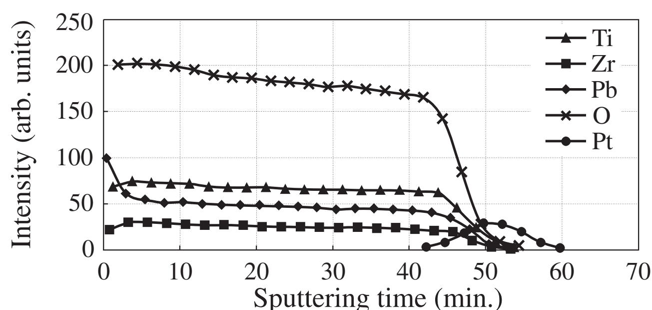

Figure 1. AES profiles of a thin PZT film deposited on Pt–quartz substrate (target: Zr/Ti = 40/60 + 10% PbO; film thickness: 0.3 μm; annealing temperature: 570 °C).

annealed, we observed a considerable increase in the Pb concentration near the top surface of the films. According to previously reported data [20], this increase may be associated with the formation of lead oxide regions.

3.1. P–V and C–V measurements

Figure 2 presents a characteristic hysteresis loop (P–V) of a film deposited by sputtering of a Zr/Ti = 54/46 stoichiometric ceramic target onto glass-ceramic–Ti–Pt substrate and annealed at 550 °C for an hour in a conventional furnace. It is clearly seen that the hysteresis loop is nearly symmetrical. Its remanent polarization is as high as 20 μC cm^{-2}.

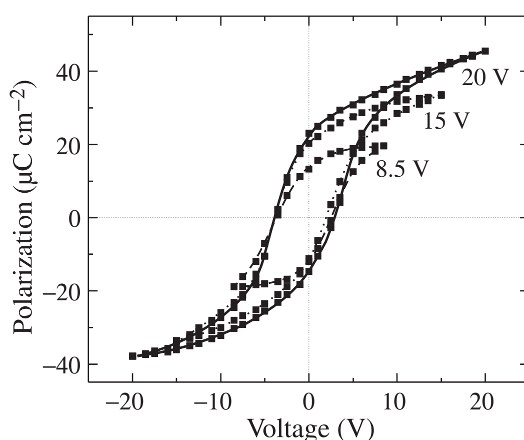

Figure 2. Hysteresis loops at different amplitudes of applied ac voltage for a thin film deposited onto a glass-ceramic–Ti–Pt substrate by sputtering of Zr/Ti = 54/46 stoichiometric ceramic target and annealed at 550 °C for 1 h; PZT film thickness: 0.5 μm (f = 50 Hz).

By contrast, the films fabricated by sputtering of a target with 10 mol% excess of PbO show a pronouncedly asymmetric hysteresis loop (figure 3(a)). This means that there is some internal electric field in this film. Moreover, we can see that the loop curve is shifted along the abscissa axis and has a distorted shape. Exactly the same asymmetric form (as for the hysteresis loop) is observed for the C–V curve (figure 4(a)). The shape of the hysteresis loop (figure 3(a)) resembles that of a poled ferroelectric ceramic with space-charge accumulation occurring during the period of aging [21]. Similarly, we can suggest that the film is self-polarized by a built-in electric field and contains a sufficient number of charge carriers.

Judging from the initial hysteresis loop, the built-in field in the film reaches a value of 35 kV cm^{-1} (figure 3(b)). There are at least two ways to decrease the asymmetry of hysteresis curves and the internal field in the PZT films. One of these is to apply a strong ac field to the sample. On applying a strong (about 300–400 kV cm^{-1}) electric field, we can obtain fully symmetrical curves. Another way to symmetrize the hysteresis loop is to anneal the sample at above 300 °C, which makes it quite symmetrical (figures 3(c), (d)). The C–V curves have a practically symmetric shape, too (figure 4(b)). However, in the course of time the hysteresis loop becomes slightly asymmetrical again (figure 3(f)), and under a weak external ac electric field the loop has a constriction (figure 3(e)).

Note that the findings obtained hold also for the films with an excess of PbO and are similar to those for films deposited on different substrates used in this work.

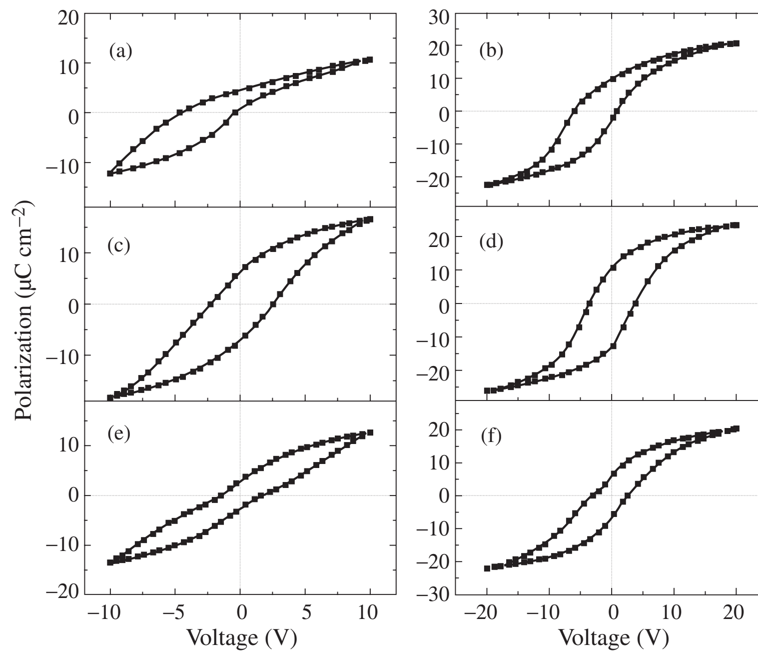

Figure 3. Hysteresis loops at applied ac voltages with amplitudes of 10 V ((a), (c), (e)) and 20 V ((b), (d), (f)) for thin films deposited onto a glass-ceramic–Ti–Pt substrate by sputtering of Zr/Ti = 54/46 + 10 mol% PbO ceramic target and annealed at 550 °C for 1 h before ((a), (b)) and immediately after thermal annealing ((c), (d)), and after 100 h of aging ((e), (f)). PZT film thickness: 0.5 μm ($f = 50$ Hz).

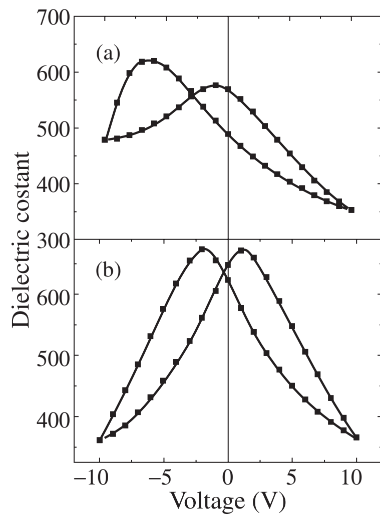

Figure 4. *C–V* characteristics of thin films deposited onto a glass-ceramic–Ti–Pt substrate by sputtering of Zr/Ti = 54/46 + 10 mol% PbO ceramic target and annealed at 550 °C for 1 h before (a) and immediately after thermal annealing (b).

3.2. LIMM and pyroelectric measurements

In all of the films studied, the pyroelectric coefficient (γ) correlates with the remanent polarization obtained from the hysteresis loops within the accuracy of the measurement. The simplest explanation of this correlation is that the polarization and pyroelectric coefficient are

proportional to the area fraction of the poled film and to the concentration of the perovskite phase. The maximal values of γ (20–24 nC cm^{-2} K^{-1}) were obtained for films grown by sputtering of a stoichiometric PZT target. The γ-value was lower and equal to 17–18 nC cm^{-2} K^{-1} for a PZT composition Zr/Ti $= 54/46 + 10$ mol% PbO, when a positive voltage (+17 V) was applied to the top electrode of the samples. Moreover, negative poling ($V = -17$ V; film thickness: 1 μm) reduced the γ-coefficient to 13–14 nC cm^{-2} K^{-1}. The difference between the coefficients $+\gamma$ and $-\gamma$ seems to be associated with the built-in electric field whose direction coincides with that of the field induced by application of +17 V. Raising the sample polarizing voltage (to more than 30 V) led to an increase in the coefficient $-\gamma$ and to equalization of the values of $+\gamma$ and $-\gamma$.

Measurements of the pyroelectric coefficient (γ_{s-p}) on self-polarized films demonstrated that γ_{s-p} does not exceed 15–20% of the coefficient measured for preliminarily polarized films. The direction of self-polarization in the films was towards the top electrode.

The results obtained in studying LIMM polarization profiles for a self-polarized film are presented in figure 5 (curve 1). It can be seen that the self-polarization is localized at the bottom electrode, with the peak of the curve lying at $x/d \approx 0.16$–0.18. It is interesting that the polarization changes its sign to the opposite near the middle of the film thickness, and the upper part of the film is weakly oppositely charged. A similar $P(x/d)$ distribution was measured for the films deposited by sputtering a Zr/Ti $= 40/60+10\%$ PbO target. The polarization profiles of preliminarily polarized PZT films differ substantially from those observed for self-polarized films. The $P(x/d)$ distribution for a film sputtered from a Zr/Ti $= 40/60+10\%$ PbO target is shown in figure 6. The sample was poled under a bias of 20 V at room temperature in the positive and negative polarization directions for 30 min. The maximum of $P(x/d)$ is strongly shifted to the bottom electrode of the structure and corresponds to $x/d \approx 0.26$–0.28. It is interesting to note that the curves for the positive and negative polarization directions are practically equivalent.

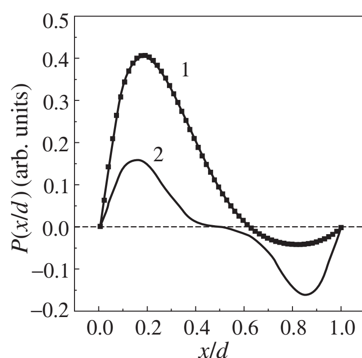

Figure 5. The polarization distribution profile $P(x/d)$ for the original self-polarized thin film (target Zr/Ti = 54/46 + 10% PbO) (curve 1) and the hypothetical curve $P(x/d)$ for the thin film after thermal treatment at 300 °C (curve 2).

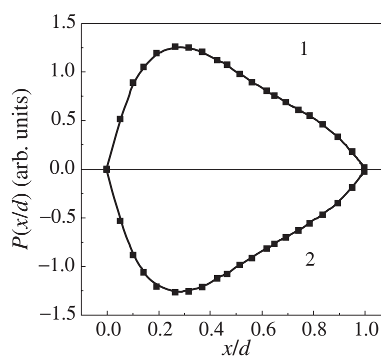

Figure 6. The polarization distribution profile $P(x)$ for a thin film (target: Zr/Ti = 40/60 + 10% PbO) deposited onto a fused silica–Pt substrate and polarized for 30 min under biases of 20 V ($+P$) and −20 V ($-P$) at room temperature.

4. Discussion

The self-polarization effect in ferroelectric films reveals itself in the course of deposition and may occur for two main fundamental reasons: the presence of a built-in electric field and the

existence of a mechanical stress. The built-in electric field in a PZT film may arise because of an asymmetric charge distribution at the interfaces [4, 10], Schottky barrier fields caused by the difference between the work functions of the electrode and ferroelectric film materials [5, 7, 8], the effect of an uncontrollable electric field existing during the process of ion-plasma deposition of the PZT film [22], the presence of donor or acceptor impurities in the PZT film [6, 23], or for some other reasons. The origin of the mechanical stress has not been explained yet. This stress may originate from the difference between the thermal expansion coefficients of the ferroelectric film, substrate and bottom electrode, or because of the formation of a perovskite phase upon thermal annealing [22]. In addition, a piezoelectric effect may affect (increase or decrease) the built-in field and the degree of self-polarization. Such a complexity makes it difficult to reveal the real reasons for self-polarization.

Experimental data on formation and modification of the built-in electric field contributing to self-polarization, obtained in this and other works, can be summarized as follows:

(a) The internal built-in field affects the P–E and C–V dependences.
(b) The presence of the built-in field is associated with the non-stoichiometry of the PZT film composition (excess of PbO) and with dopants.
(c) The built-in field is formed mainly at the bottom Pt–PZT interface after the perovskite phase has crystallized in the PZT film.
(d) The direction of self-polarization (towards bottom or top electrodes) in the capacitor structure depends on a number of technological factors.
(e) The restoration of the symmetry of P–E and C–V dependences by application of a strong external electric field or by thermal treatment shows that the direction and amplitude of the built-in electric field can be varied.

In-depth analysis proves the influence of free carriers on how the internal (built-in) electric field sets up in ferroelectric films. Carriers commonly appear as a result of deviations of the ferroelectric film composition from stoichiometry and the presence of dopants and contaminants. For instance, addition of only 5 mol% niobium (Nb^{5+}) to PZT gives rise to a 40 kV cm^{-1} built-in electric field shifting the hysteresis loop to the negative fields (the electric field direction is towards the bottom interface). The fact that the built-in field increases in proportion to the niobium dopant concentration is particularly remarkable [24].

In accordance with the results of recent investigations, self-polarization arises without any special doping. It is well known that in lead-based ferroelectrics with non-stoichiometric concentrations of lead and oxygen, the charge carriers are lead or oxygen vacancies [20, 25]. Such a situation is the rule rather than the exception for PZT films. The reason is that the film is deposited onto a hot substrate and a certain amount of lead evaporates from the substrate owing to the high diffusivity of lead and the volatility of lead oxide vapour. To compensate for the loss of lead, the sputtered target usually contains an excess of lead oxide.

For the stoichiometric target composition, the effect of self-polarization is commonly less pronounced if the deposition process does not substantially change the stoichiometry of a deposited film. A similar situation is observed in the present work with films deposited by magnetron sputtering of a stoichiometric target and onto a substrate kept at low temperature (130 °C) then annealed at 520–550 °C [14]. For these films, the hysteresis loop shows minimum deviations from the symmetric form (figure 2).

The excess lead in the sputtered target (10 mol% PbO) gives rise to a built-in field, and the hysteresis loop is shifted to negative fields. This proves the presence of a negative charge at the interface between the film and the bottom electrode. A similar shift was observed in some other works [6, 10, 12, 24].

In our opinion, the self-polarization effect may be caused by two factors: (i) the n-type PZT film conductivity due to the presence of the oxygen vacancies and (ii) a very high density of trap states at the bottom Pt/PZT interface. The formation of the oxygen vacancies is due to the excess lead in the film, extracting mobile oxygen from the perovskite matrix in oxidation. In the case in question, the presence of lead oxide near grain boundaries and structure interfaces is explained by the migration of Pb ions towards the boundaries of perovskite crystallites in the course of thermal treatment [25]. In addition, various defects, mainly incorporating oxygen vacancies, may appear during perovskite phase formation in high-temperature annealing [20].

The high density of trap states at the bottom interface is due to the interdiffusion and chemical reactions between the electrode and ferroelectric material during annealing [6, 9–11]. The interface becomes an area of spontaneous formation of negative charge, transforming the PZT film into a polar state in the vicinity of the boundaries, with the polarization vector directed towards the bottom electrode and the hysteresis loop (figure 3(a)) and C–V characteristics (figure 4(a)) shifted to the left. It is the negative charge that appears at the film–electrode interfaces owing to the higher density of states filled by electrons from the n-type PZT.

Negative charge may be formed at the top interface owing to the high density of electron traps in this region. However, the conditions of top-electrode deposition (Pt sputtering at 150 °C) may preclude the appearance of any substantial negative charge at the top interface. This assumption is confirmed by a polarization-profiling curve in figure 5 (curve 1). It can be seen that the directions of polarization at the top and bottom interfaces are opposite, owing to the negative charge accumulation in these regions, with the polarization more pronounced at the bottom electrode. An energy diagram leading to self-polarization at both the bottom and the top interfaces of a thin PZT film is shown schematically in figure 7(a).

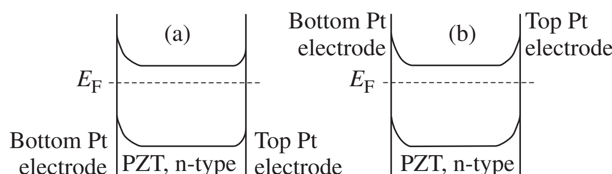

Figure 7. Energy band diagrams for n-type PZT capacitor with top and bottom Pt electrodes for the original self-polarized PZT thin film containing an excess of PbO (a) and the same film after thermal annealing at 300 °C (b).

It should be emphasized that migrating charges play a twofold role in the appearance of self-polarization. Firstly, being concentrated at the interfaces, the charges (electrons) form built-in fields polarizing the ferroelectric film; secondly, the charges screen the spontaneous polarization, forming the migratory polarization [21]. In other words, the process in which self-polarization and migratory polarization are formed is self-consistent. So, by finding the internal field from the P–V and C–V curves, we actually determine the field of migratory polarization, the charge migration process being rather slow. In contrast, in LIMM measurements performed in the short-circuit mode, the field of migratory polarization is not revealed.

It should be noted that varying the content of excess lead may result in a redistribution of the density of charged states at both the interfaces, with oppositely directed built-in field and self-polarization, as observed in PLZT films [6]. In our opinion, the positive charging of the bottom interface and the corresponding positive shift (to the right) of the hysteresis loops [2–6] are caused by Pb deficiency in the perovskite lattice and formation of lead vacancies with acceptor properties. This is a common situation with piezoceramics, described in detail

elsewhere [25]. In this case, raising the PbO content of the sputtered target may lead to charge-carrier inversion in PLZT films, accompanied by charge inversion of the surface states and inversion of the built-in field direction at the interfaces.

The model of the Schottky barrier at the ferroelectric film–electrode interfaces seems to be not quite correct, as it takes no account of the high density of states at the interfaces and fails to explain the origin of the experimentally observed high internal bias fields.

The assumption that charged traps give rise to the built-in field at the Pt–PZT interface is supported by the results of capacitor structure thermal treatment (figures 3(c)–(f)). The destruction of the built-in field and self-polarization upon thermal treatment suggests that the charge redistribution between the top and bottom interfaces is closely associated with the trap state density at the interfaces. Annealing this structure at 300–400 °C results in a rather high trap density at the top platinum–film interface and in relaxation of a substantial charge occupying these trap states. The hysteresis loops become symmetric in both strong and moderate electric fields (figures 3(c), (d)). The same is observed for the C–V characteristics (figure 4(b)).

If the trap state densities at the two interfaces are equal, the majority carriers (electrons) are distributed with equal probabilities between the top and bottom interfaces of the capacitor structure. They are localized near both the interfaces, and the field (and polarization) vectors are oppositely directed at the interfaces (see figure 5, curve 2, and figure 7(b)).

After thermal treatment, free charges are gradually captured by local surface trap states. This process gives rise to an electric field, with the corresponding self-polarization occurring at the interfaces. In this case, the shape of the hysteresis loop in moderate fields (figure 3(e)) is a sum of two symmetrically inverted loops of the type shown in figure 3(a) and has a constriction in the case of equal built-in fields at the interfaces. The hysteresis loops take a classic shape in strong electric fields (figure 3(f)). No macroscopic polarization is observed (figure 5, curve 2). A similar situation was described by Okazaki for strong piezoceramics influenced by the migratory polarization induced by the presence of donor and acceptor impurities [21].

As mentioned above, applying a strong ac field (up to 400 kV cm^{-1}) leads to a redistribution of the surface state charges at the top and bottom interfaces, with the hysteresis loops becoming symmetric. However, in contrast to the effect of thermal treatment of the capacitor structure, spontaneous charge redistribution occurs gradually on switching the ac field off, in agreement with the densities of states at the interfaces. That is why the built-in electric field and the self-polarization at the bottom interface are restored practically to their initial values.

The asymmetry of the profiles ($+P$ and $-P$) of the polarization distribution across the thickness of a poled PZT film (see figure 6) indicates that a higher trap state density can be found at the bottom Pt–PZT interface, rather than at the top one. This is quite evident for the case when the direction of the poling external field coincides with that of the built-in field. If the poling field is opposite to the built-in field, then the bottom interface will have no negative charges but will be charged by positive charge carriers that also exist in the film volume.

5. Conclusions

We have shown that:

(a) Integrated studies of the hysteresis loops and C–V curves, together with determining the polarization distribution across the film by the LIMM, allowed us to establish relationships between the technological parameters of film processing and physical properties of PZT thin films and develop the concept of the self-polarization effect.

(b) The source of self-polarization is the bottom interface of the thin-film Pt–PZT–Pt capacitor structure fabricated with a certain sequence of structure formation.

(c) The self-polarization effect is caused by two factors which are, first, the n- or p-type conduction by oxygen or lead vacancies, or other impurities in the films, and, second, the higher trap density at the bottom interface of the structure, compared with that at the top interface, determined by the different conditions of interface formation.

References

[1] Adachi M, Matsuzaki T, Yamada N, Shiosaki T and Kawabata A 1987 *Japan. J. Appl. Phys.* **26** 550

[2] Kochler R, Neumann N, He Z, Bruchhaus R, Wersing W and Simon M 1997 *Ferroelectrics* **201** 83

[3] Schreiter M, Bruchhaus R, Pitzer D and Wersing W 1998 *Proc. ISAF XI '98: 11th IEEE Int. Symp. on Applications of Ferroelectrics (Montreux, Switzerland, 24–27 August 1998)* (New York: IEEE) pp 181–5

[4] Gerlach G, Suchaneck G, Kochler R, Sandler T, Padmini P, Krawietz R, Pompe W, Frey J, Jost O and Schonecker A 1999 *Ferroelectrics* **230** 109

[5] Kholkin A L, Brooks K G, Taylor D V, Hiboux S and Setter N 1998 *Integrated Ferroelectr.* **22** 525

[6] Kobune M, Ishito H, Mineshige A, Fujii S, Takayama R and Tomozawa A 1998 *Japan. J. Appl. Phys.* **37** 5154

[7] Scott J F, Watanabe K, Hartmann A J and Lamb R N 1999 *Ferroelectrics* **225** 83

[8] Lee J J, Thio C I, Bhattacharya M and Desu S B 1995 *Mater. Res. Symp. Proc.* **361** 241

[9] Bell J M, Knight P C and Johnston G R 1996 *Ferroelectric Thin Films: Synthesis and Basic Properties* ed C Paz de Araujo, J F Scott and G W Taylor (London: Gordon and Breach) p 93

[10] Okamura S, Miyata S, Mizutani Y, Nishida T and Shiosaki T 1999 *Japan. J. Appl. Phys.* **38** 5364

[11] Song Z-T, Ren W, Zhang L-Y and Lin Ch 1999 *Thin Solid Films* **353** 25

[12] Wang Z-J, Maeda R and Kikuchi K 1999 *Japan. J. Appl. Phys.* **38** 5342

[13] Afanasjev V P, Kaptelov E Yu, Kramar G P, Pronin I P and Shaplygina T A 1994 *Phys. Solid State* **36** 906

[14] Afanasjev V P, Bogachev S V, Zaitseva N V, Kaptelov E Yu, Kramar G P, Petrov A A and Pronin I P 1996 *Tech. Phys.* **41** 607

[15] Lang S B 1990 *Ferroelectrics* **106** 269

[16] Lang S B 1991 *Ferroelectrics* **118** 343

[17] Suchaneck G, Sandler Th, Kochler R and Gerlach G 1999 *Integrated Ferroelectr.* **27** 127

[18] Suchaneck G *et al* 1998 *Proc. ISAF XI '98: 11th IEEE Int. Symp. on Applications of Ferroelectrics (Montreux, Switzerland, 24–27 August 1998)* (New York: IEEE) p 187

[19] Pronin I P, Zaitseva N V, Kaptelov E Yu and Afanasjev V P 1997 *Izv. Akad. Nauk Ser. Fiz.* **61** 379

[20] Yamakawa K, Arisumi O, Okuwada K, Tsutsumi K and Katata T 1998 *Proc. ISAF XI '98: 11th IEEE Int. Symp. on Applications of Ferroelectrics (Montreux, Switzerland, 24–27 August 1998)* (New York: IEEE) p 159

[21] Okazaki K 1969 *Ceramic Engineering for Dielectrics* (Tokyo: ?)

[22] Sviridov E, Sem I, Alyoshin V, Biryukov S and Dudkevich V 1995 *Mater. Res. Soc. Symp. Proc.* **361** 141

[23] Fujisawa H, Nakashima S, Kaibara K, Shimizu M and Hiu H 1999 *Japan. J. Appl. Phys.* **38** 5292

[24] Klissurska R D, Tagantsev A K, Brooks K G and Setter N 1995 *Microelectron. Eng.* **29** 271

[25] Xu Yu 1991 *Ferroelectric Materials and their Applications* (Amsterdam: North-Holland) 391 pp